Available online at www.sciencedirect.com
ScienceDirect
Journal of Environmental Sciences 21(2009) 1525–1531
JOURNAL OF ENVIRONMENTAL SCIENCES
ISSN 1001-0742
CN 11-2629/X
www.jesc.ac.cn

Chemical composition and size distribution of secondary organic aerosol formed from the photooxidation of isoprene

LIU Xianyun, ZHANG Weijun*, WANG Zhenya, ZHAO Weixiong, TAO Ling, YANG Xibin

Laboratory of Environmental Spectroscopy, Anhui Institute of Optics and Fine Mechanics, Chinese Academy of Sciences, Hefei 230031, China. E-mail: xianyunliu@gmail.com

Received 18 January 2009; revised 18 May 2009; accepted 27 May 2009

Abstract

Photooxidation of isoprene leads to the formation of secondary organic aerosol (SOA). In this study, the chemical composition of SOA formed from OH-initiated photooxidation of isoprene has been investigated with gas chromatography/mass spectrometry (GC/MS) and a home-made aerosol time-of-flight mass spectrometer. Sampling particles generated in a home-made smog chamber. The size distribution of SOA particles was detected by a TSI 3321 aerodynamic particle size spectrometer in real time. Results showed that SOA created by isoprene photooxidation was predominantly in the form of fine particles, which have diameters less than 2.5 μm. The obtained mass spectra of individual particles show that products of the OH-initiated oxidation of isoprene contain methyl vinyl ketone, methacrolein, formaldehyde, and some other hydroxycarbonyls. The possible reaction mechanisms leading to these products were also discussed.

Key words: secondary organic aerosols; isoprene; aerosol time-of-flight mass spectrometer; smog chamber; size distribution

DOI: 10.1016/S1001-0742(08)62450-X

Introduction

Isoprene (2-methyl-1,3-butadiene) is an important biological material, and can be a harmful environmental pollutant and toxicant when present in excess quantities (Sanadze, 2004). It is found to emit in large quantities from numerous plant species during daylight hours and estimated global emission was about 500 Tg/year (Guenther *et al*., 1995). Isoprene can form secondary organic aerosols (SOA) through photooxidation with OH radicals, NO_3 radicals, and O_3, in which OH radical reaction is dominate during daytime (Thomas *et al*., 2008). The conversion process can increase the ozone concentration in troposphere as well as the formation of SOA (Odum *et al*., 1997), and SOA formation in the atmosphere can adversely affect visibility (Pilinis *et al*., 1995), the climate (Annmarie *et al*., 1993), and human health (Schwartz *et al*., 1996). To reduce these impacts, control strategies are required to reduce their ambient concentrations, and knowledge of isoprene oxidation products is required. Several detection methods have been used to study the formation mechanism, and many techniques were used to study the chemical composition of SOA particles formed from the photooxidation of isoprene, including gas chromatograph/mass spectrometer (GC-MS) (Claeys *et al*., 2004; Surratt *et al*., 2006), liquid chromatograph/electrospray mass spectrometer (LC/ESI-MS), matrix-assisted laser desorption ionization-time of flight mass spectrometer (MALDI-TOFMS), aerosol mass spectrometry (AMS) (Kroll *et al*., 2006), atmospheric pressure ionization tandem mass spectrometer (API MS) (Kwok *et al*., 1995), electrospray ionization (ESI), and gas chromatography/ion trap mass spectroscopy (GC/ITMS) (Yu *et al*., 1995; Szmigielski *et al*., 2007). In addition, the Fourier transform infrared (FT-IR) spectrometry was used to obtain additional information of functional group for SOA products formed from the photooxidation of isoprene (Ruppert and Becker, 2000; Jang *et al*., 2002). However, these methods often use off-line techniques, the SOA particles are usually collected by filters or impact plate, and there are some disadvantages in GC/MS and CI-GC-ITMS systems, for example, possible secondary chemical reactions or loss of semivolatile compounds associated with traditional aerosol sampling onto a filter or impact plate, or with multi-step chemical treatments, and it is difficult to measure the size and chemical compositions of individual SOA particles simultaneously.

The aerosol time-of-flight mass spectrometer (ATOFMS) has been designed to sample single aerosol particles in real time (Noble and Prather, 1996; Gard *et al*., 1997). This instrument has been remarkably used for sampling ambient atmospheric aerosols and has been used in many other applications. Most of the instruments can size, count, and mass-analyze individual particles with high time-resolution.

In this work, we initiated the photooxidation of isoprene

* Corresponding author. E-mail: wjzhang@aiofm.ac.cn

by OH radical to form SOA in a home-made smog chamber, and used GC/MS, ATOFMS and TSI 3321 to investigate the formation of SOA particles. The positive mass spectra of SOA particles from photooxidation of isoprene were obtained, the diameter of individual particle, number distribution of SOA particle diameter, and molecular composition of SOA particle were measured.

1 Experiment

1.1 Smog chamber experiment

Isoprene (99%) (CAS #78-79-5) was obtained from Alfa Aesar, Johnson Matthey Company (USA); sodium nitrate (> 99%) and methanol (> 99%) were purchased from the Third Reagent Manufactory (Tianjin, China); and nitrogen oxide (99.9%) obtained from Nanjing Special Gas Factory, (China). All those chemicals were used without further purification.

Methyl nitrite was synthesized by dropping sulfuric acid into a methanol solution of sodium nitrate. The reaction products passed through saturated sodium hydroxide trap to remove the traces of sulfuric acid, dried by passing through a calcium sulfate trap, and collected using a condenser of liquid nitrogen at 77 K. The methyl nitrite was purified using a vacuum system of glass.

Photooxidation of isoprene was performed using UV-irradiation of isoprene/CH_3ONO/NO/air mixtures in an indoor photochemical smog chamber. The detail information of facilities was given elsewhere (Hao *et al*., 2005). In brief, the experimental apparatus consists of a sampling system, a smog chamber system and detecting system. The smog chamber was made of sealed collapsible polyethylene with a volume of 850 L, and the ratio of surface to volume was 5.8 m^{-1}. It is surrounded by twelve 20-W fluorescent black lamps to initiate the reaction, each black lamp with UV radiation wavelength of 300–400 nm.

Before each experiment, the chamber was flushed continuously with dry purified laboratory compressed air for 20 min. The compressed air was processed through three consecutive packed-bed scrubbers, containing activated charcoal, silica gel and a Balston DFU® filter (Grade BX), to remove the trace of hydrocarbon compounds, moisture and particles. Isoprene was sampled by a micro liter injector and injected directly into the chamber. NO and methyl nitrate were expanded into the evacuated manifold to the desired pressure through Teflon lines, and introduced into the smog chamber by a stream of purified air. The whole system was completely shrouded from light with a black polyethylene tarpaulin. Hydroxyl radicals were generated by the photolysis of methyl nitrite in air at wavelengths longer than 300 nm (Atkinson *et al*., 1981). The chemical reactions leading to the formation of OH radical are as the following Eqs. (1)–(3):

$$CH_3ONO + h\upsilon\ (\lambda > 300\ \text{nm}) \longrightarrow CH_3O\cdot + NO \quad (1)$$

$$CH_3O\cdot + O_2 \longrightarrow HCHO + HO_2\cdot \quad (2)$$

$$HO_2\cdot + NO \longrightarrow \cdot OH + NO_2 \quad (3)$$

After the injection of reactants into the smog chamber, purified air was added into the chamber again until the pressure reached 10^5 Pa. Then, reaction was initiated by irradiating the chamber with black lamps. During all the experiments, the relative humidity was in the range of 50%–70%, and the temperature was (295 ± 2) K. The size distribution, the number concentration and the mass concentration of SOA particles were detected by a TSI 3321 aerodynamic particle size spectrometer (USA) in real time.

1.2 Aerosol time-of-flight mass spectrometer (ATOFMS)

ATOFMS is a home made single particle mass spectrometer, which is designed to sample individual aerosol particle in real time. It includes an aerosol introduction interface, a light scattering region for particle detection and velocity/size determination, and a linear-time-of-flight mass spectrometry for single particle composition analysis (Xia *et al*., 2004a, 2004b). Particles are sampled through a converging nozzle. The nozzle is separated from a skimmer and the region is mechanically pumped to a pressure of 267 Pa. The particles are accelerated to a terminal velocity which is proportional to their aerodynamic size. A secondary skimmer allows for differential pumping to reach the pressures needed to operate the mass spectrometer and collimates the particle beam by removing the particles that do not follow a straight trajectory through the nozzle. Particles then enter the light scattering region where they encounter two red continuous-wave, diode-pumped lasers separated by a known distance. The lasers are positioned perpendicular to one another and orthogonal to the particle beam. For each laser, an arrangement of optics is used to focus the laser beam to a spot that intersects the particle beam. A particle passing through each laser beam scatters light, which is collected by an ellipsoidal mirror and focused onto a photomultiplier tube (PMT) detector. PMTs send pulses to an electronic timing circuit that measures the time required for the particle to travel the known distance between the two scattering lasers. The distance and the particle time-of-flight are used to calculate the particle velocity. An external size calibration uses particles of known size to relate the velocity to a physical aerodynamic diameter. Then the circuit begins a countdown to the time when the particle reaches the center of the ion source region of a mass spectrometer. At the same time, the circuit sends a signal to fire a pulsed excimer KrF laser at 248 nm, having an average power density of 1×10^7 W/cm^2 and a pulse length 2.5 ns. Upon absorption of the laser pulses, the particle is heated in a rapid fashion, desorbing and ioning individual molecules from the particle. The resulting ions are mass analyzed in a linear time-of-flight mass spectrometer. Thus, for each particle analyzed, the size is obtained through the particle velocity, and the corresponding particle composition is determined through the positive ion mass spectra.

1.3 Gas chromatography/mass spectrometry (GC/MS)

The mixtures were irradiated by 8 black lamps for 1.5 h. At the end of the reaction, the SOAs produced by the

photooxidation were captured with CH_2Cl_2 washing bottle for 1 h through a Balston DFU® filter and a 5 L/min air extracting pump. The aerosol samples were subjected to the analysis of GC/MS. A schematic diagram of the experimental system is shown in Fig. l.

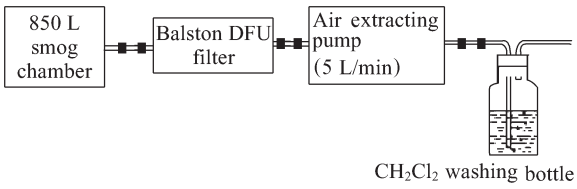

Fig. 1 Schematic of the experimental apparatus.

GC/MS analyses were performed on an Agilent 6890/micromass GCT-MS system (USA). A DB-5MS fused-silica capillary column (0.25 μm film thickness, 30 m × 0.25 mm i.d.) was used to separate the derivatized extracts. Helium was used as carrier gas at a flow rate of 1.5 mL/min. The temperature program was as follows: isothermal hold at 80°C for 2 min, temperature ramp of 15°C/min up to 280°C. The analysis was performed in the mass range of 30–400 amu, and was carried out in the electron ionization (EI) mode. The ion source was operated at electron energy of 70 eV at 250°C. The GC re-entrant temperature and inlet temperature were 250 and 280°C, respectively.

2 Results and discussion

With the above mentioned experimental conditions, the mixing ratio of CH_3ONO, isoprene, and NO is 20, 2, and 2 ppmv, respectively. The diameter of individual particles, size distribution and molecular composition of SOA particle were obtained.

2.1 Chemical composition of SOA particles

Figure 2 presents a GC/MS total ion chromatogram (TIC) obtained for SOA formed from the isoprene photooxidation. The corresponding EI mass spectra are shown in Fig. 3. Isoprene hydroxyperoxy (RO_2) radicals were found to elute from the GC column at 5.31 and 5.43 min, the corresponding EI spectra for these peaks are shown in Figs. 3a and 3b, respectively. The C_5 alkene triols, such as *cis*-2-methyl-1,3,4-trihydroxy-1-butene, 3-methyl-2,3,4-trihydroxy-1-butene, and trans-2-methyl-1,3,4-trihydroxy-1-butene, are shown in Fig. 3c. 2-Methylglyceric acid (2-MG) monomer $C_4H_8O_4$ (*m/z* = 120) was detected in the experiment and the EI spectrum is shown in Fig. 3d. Figure 3e shows a mass spectrum recorded for the largest chromatographic peak (RT = 6.97 min) from the EIC, which is assigned to 2-MG dimer.

Figure 4 shows a positive mass spectrum collected using the ATOFMS instrument for the SOA particles of $CH_3ONO/NO/isoprene/air$ mixture. The mass spectrum of the irradiated $CH_3ONO/NO/isoprene/air$ mixture showed weak ion peaks at *m/z* = 70 (Fig. 4), which is due to the methyl vinyl ketone and methacrolein, known products

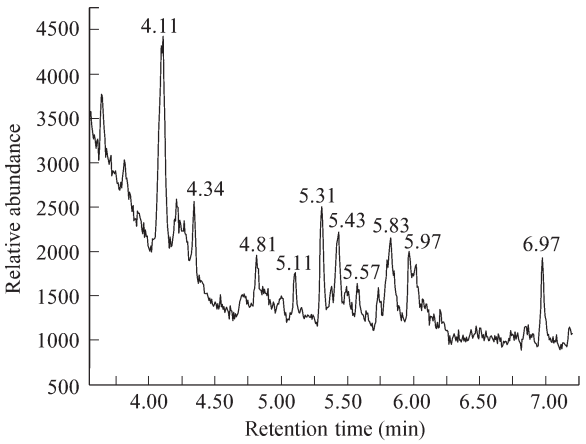

Fig. 2 GC/MS total ion chromatogram (TIC) of isoprene photooxidation products.

of the OH radical-initiated reaction of isoprene (Tuazon and Atkinson, 1990; Paulson *et al*., 1992; Miyoshi *et al*., 1994). The strong peak at *m/z* = 44 is attributed to the CO_2^+ fragment, and the $(M+H)^+$ acetaldehyde. Therefore, many of the particles produced from the photooxidation of isoprene may be attribute to a single product of *m/z* = 44. The peak at *m/z* = 85 is due to addition of OH to the carbon-carbon double bonds or the initial OH radical substituent of the H at 1, 4 carbon position of isoprene, leading to the production of four hydroxyalkyl radical (Stevens *et al*., 2000). The strong peak at *m/z* = 61 is appointed to the CH_3ONO.

As shown in Fig. 4, additional prominent ion peaks are observed in the ATOFMS spectra of reacted isoprene, including those at 18, 27, 31, 120, 122 and 136. The reaction products of isoprene are given as follows:

$$OH + CH_2{=}C(CH_3)CH{=}CH_2 \longrightarrow HOCH{=}C(CH_3)CH{=}CH_2 \quad (4)$$

$$HOCH{=}C(CH_3)CH{=}CH_2 + O_2 \longrightarrow HOCH_2C(O_2)(CH_3)CH{=}CH_2 \quad (5)$$

$$HOCH_2C(O_2)(CH_3)CH{=}CH_2 + NO \longrightarrow HOCH_2C(O)(CH_3)CH{=}CH_2 + NO_2 \quad (6)$$

$$HOCH_2C(O)(CH_3)CH{=}CH_2 \longrightarrow CH_2OH + CH_3C(O)CH{=}CH_2 \quad (7)$$

$$CH_2OH + O_2 \longrightarrow HCHO + HO_2 \quad (8)$$

$$HO_2 + NO \longrightarrow OH + NO_2 \quad (9)$$

$$NO_2 + h\upsilon \longrightarrow O + NO \quad (10)$$

$$O + O_2 \longrightarrow O_3 \quad (11)$$

2.2 Mechanism for SOA formation from isoprene photooxidation

Oxidation reactions of isoprene are initiated by an attack from OH addition to the >C=C< bonds, yielding four possible hydroxyalkyl radicals, and hydroxyalkyl radicals react immediately with oxygen molecules to form eight possible hydroxyalkyl peroxy radicals. In the presence of nitric oxide (NO), the subsequent reaction of hydroxyalkyl peroxy radicals leads to the formation of

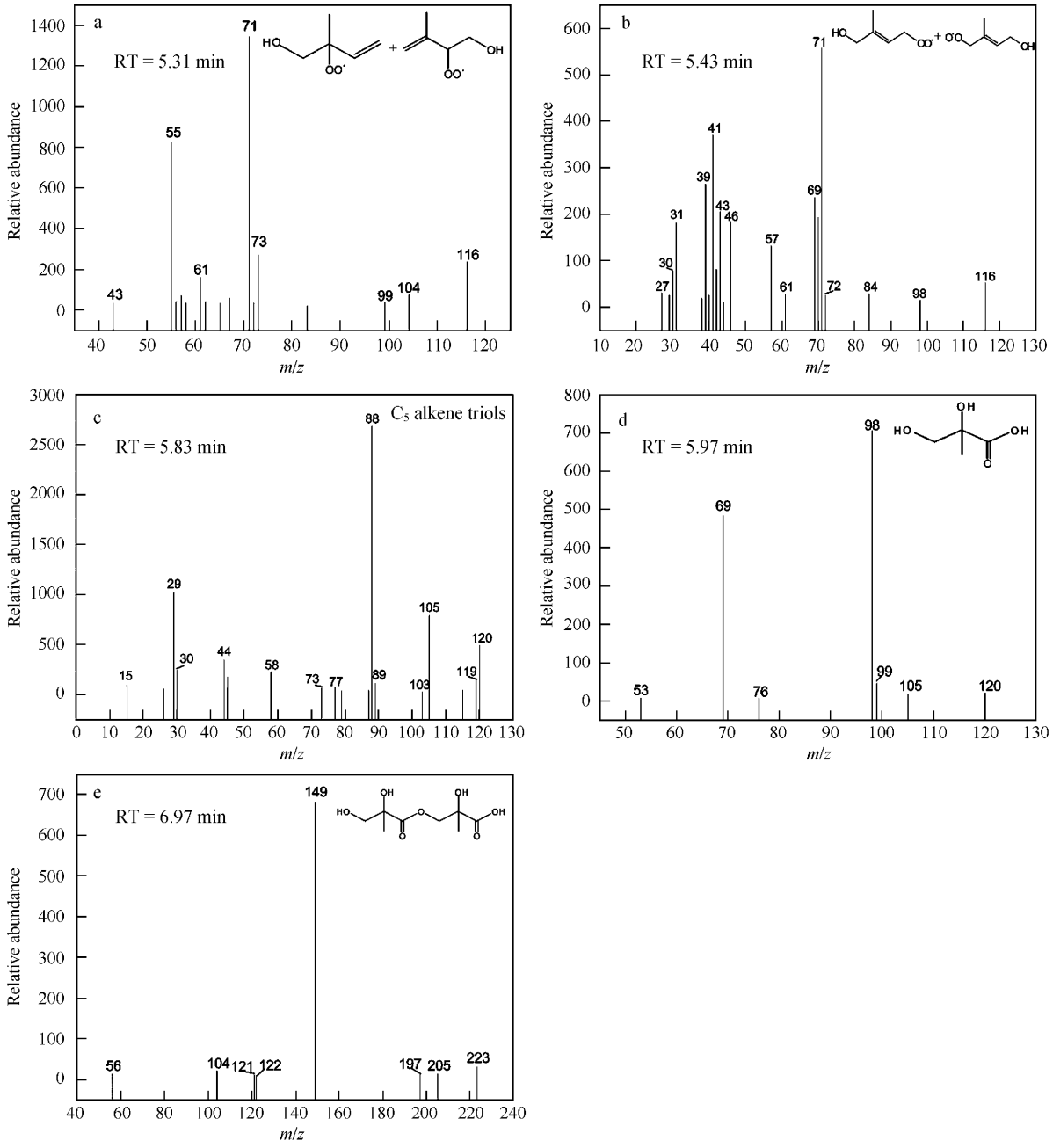

Fig. 3 EI mass spectra for the chromatographic peak from Fig. 2 identified as: (a) isoprene hydroxyperoxy radicals, OH, O_2 addition to C_1, C_2 or C_3, C_4 position; (b) isoprene hydroxyperoxy radicals, OH, O_2 addition to C_1, C_4 position; (c) C_5 alkene triols (*cis*-2-methyl-1,3,4-trihydroxy-1-butene, 3-methyl-2,3,4-trihydroxy-1-butene, and *trans*-2-methyl-1,3,4-trihydroxy-1-butene); (d) 2-methylglyceric acid monomer; (e) 2-methylglyceric acid dimer.

several major reaction products, including methyl vinyl ketone, methacrolein (MACR), formaldehyde, and organic nitrates. In the presence of NO, further oxidation will form 2-methylglyceric (2-MG) acid monomer, and 2-MG monomers can react intermolecularly to produce 2-MG acid dimer. The formation mechanism for SOA formation from isoprene photooxidation is shown in Fig. 5.

2.3 Size distribution of SOA particles

The ATOFMS instrument, sampling through the nozzle inlet, is known to have size-dependent transmission of particles into the instrument. Particle detection efficiency is an important parameter for evaluating the performance of the ATOFMS, this parameter depends on the performance of the sampling inlet and the components used for light scattering measurement, as well as on the particle size, shape, and chemical composition.

As described in the experimental section, an external timing circuit sends a triggering pulse to fire the KrF laser when the sized particle arrived the ion source region of the ATOFMS. In general, not all sized particles can produce mass spectra. In this work, hit rate of the particles, R_H, is defined as the ratio between the number of particles hit by the LDI laser, which generate ions detectable by the mass

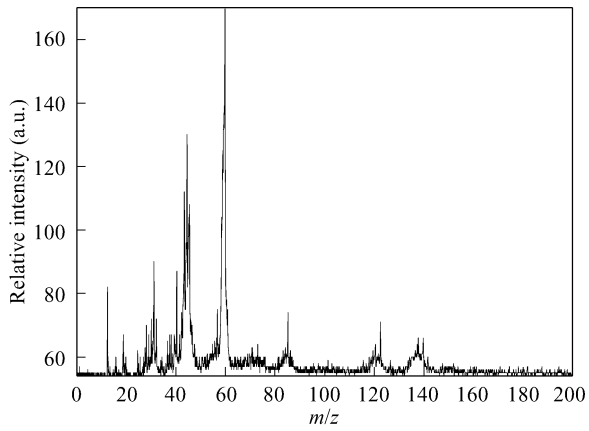

Fig. 4 Positive ATOFMS spectra of the SOA particles.

spectrometer (N_H) and the number of particles sampled by the ATOFMS during the same time period (N_S) (Eq. (12)):

$$R_H = N_H/N_S \quad (12)$$

Hit rate R_H is an important parameter for evaluating the performance of ATOFMS. It depends on the performance of the sampling inlet and the components used for light-scattering measurement, as well as on the particle size, shape, and chemical composition.

Figure 6 shows the size distribution of the sized and hit particles as well as the variation of particle detection efficiency during isoprene photooxidation experiment for 1.5 h after lights were turned on. As shown in Fig. 6, the detection efficiency is relatively uniform for isoprene SOA particles in the range of 800–1400 nm, but decreased nearly to zero out of this range. The R_H obtained in this experiment is 49%. Figure 6 also shows that the SOA particles created by isoprene photooxidation experiment

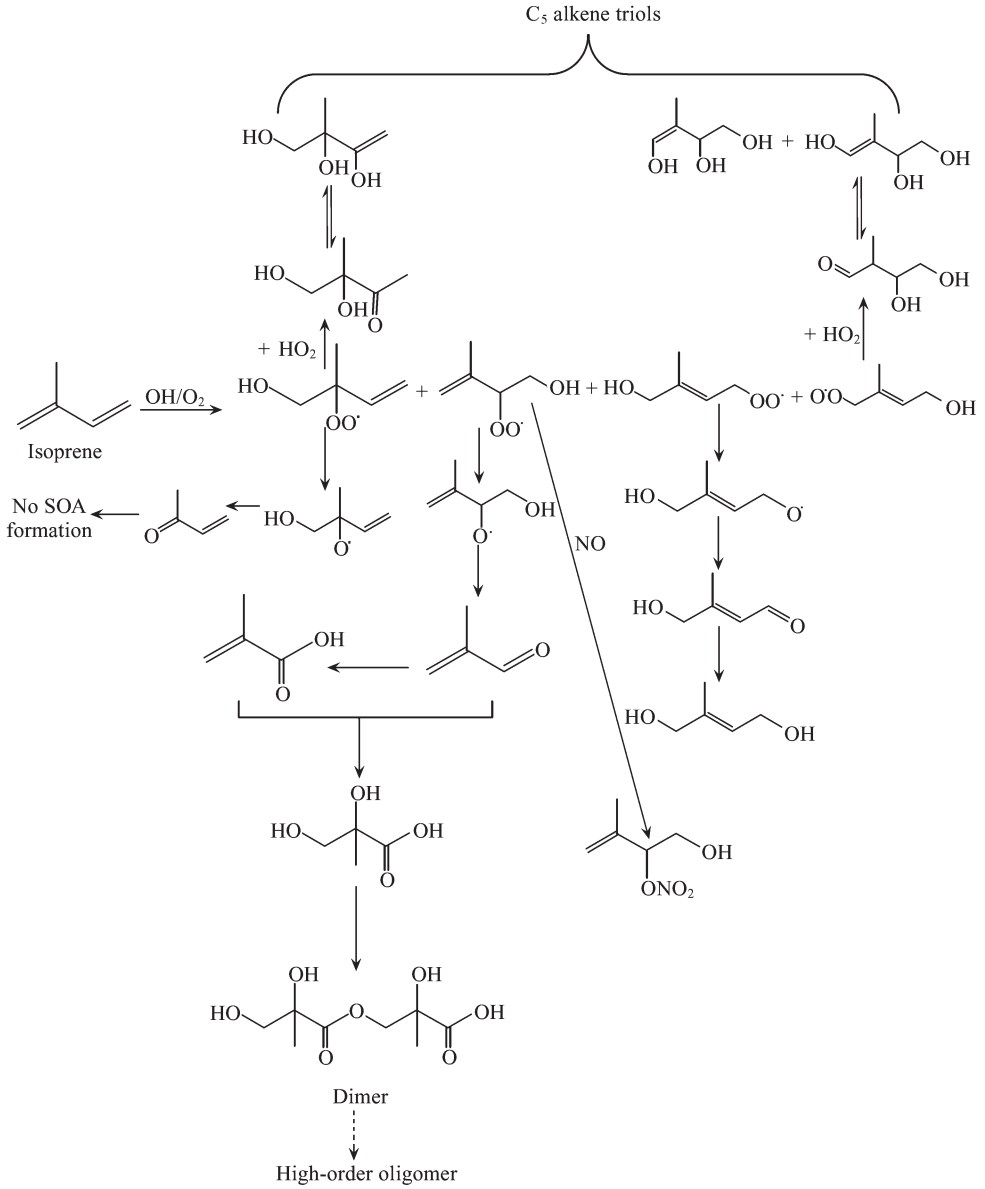

Fig. 5 Mechanism of isoprene oxidation in the presence of NO.

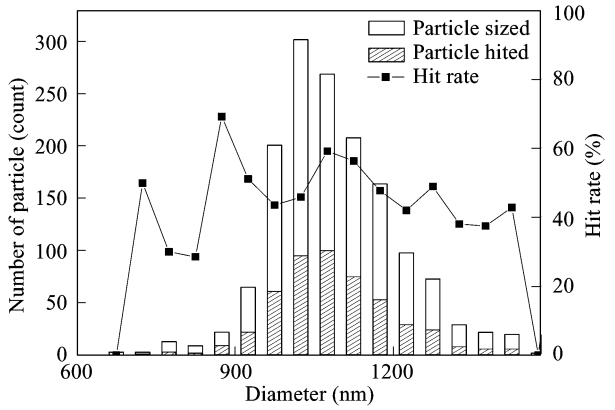

Fig. 6 Detection efficiency and number distribution of CH_3ONO/NO/isoprene/air mixture SOA particles plotted as a function of particle aerodynamic size.

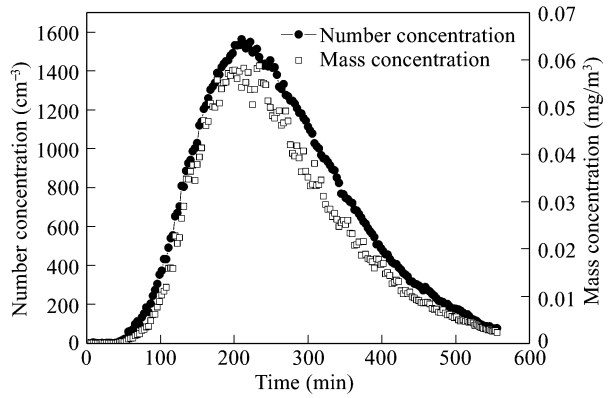

Fig. 7 Reaction profile of isoprene photooxidation experiment.

are predominant in the form of fine particles, which have diameter (0.8–1.4 μm), being less than 2.5 μm (i.e., $PM_{2.5}$). Scientific research works have proved that these fine particles are easily deposit in the lung, and do great harm to human health (Schwartz *et al*., 1996).

Figure 7 shows the dependence of both number and mass concentration of SOA particles on the light application time during the isoprene 8 black lamps photooxidation experiment. Particles are detected after about 40 min of irradiation. Aerosol growth is measured using TSI 3321 and occurs mostly after all the isoprene has been reacted. As shown in Fig. 7, both the number and mass concentration have an initial period of aerosol growth, after about 200 min of reaction, aerosol mass and volume are observed to decrease rapidly to low final values. The loss of aerosol mass stops immediately when the light is turned off, therefore, the decrease is not a result of the loss of particles to the walls. It is characterized by a shrinking of the aerosol size distribution rather than a decrease in number concentration.

3 Conclusions

The secondary organic aerosol products from photooxidation of isoprene were carried out in a smog chamber. Using GC/MS, ATOFMS, and TSI 3321 instruments, the size distribution and composition of the SOA were simultaneously detected. The mass spectra of individual particles were obtained, and results showed that products of the OH-initiated oxidation of isoprene contained methyl vinyl ketone, methacrolein, formaldehyde, 2-MG monomers, 2-MG acid dimer, and some other hydroxycarbonyls. This study clearly demonstrated that the number and mass concentration of SOA particles were increasing with the prolonging of the reaction time, and that SOA created by isoprene photooxidation was predominantly in the form of fine particles with diameters less than 2.5 μm.

Acknowledgments

This work was supported by the Knowledge Innovation Foundation of Chinese Academy of Sciences (No. KJCX2-YW-N24).

References

Annmarie E, Susan M L, Jeffrey R H, Kevin J H, Glen R C, 1993. Development of an improved image processing based visibility model. *Environmental Science and Technology*, 27(4): 626–635.

Atkinson R, Carter W P L, Winer A M, 1981. An experimental protocol for the determination of OH radical rate constants with organics using methyl nitrite photolysis as an OH radical source. *Journal of Air Pollution Control Association*, 31(10): 1090–1092.

Claeys M, Graham B, Vas G, Wang W, Vermeylen R, Pashynska V *et al*., 2004. Formation of secondary organic aerosols through photooxidation of isoprene. *Science*, 303(5661): 1173–1176.

Gard E E, Mayer J E, Morrical B D, Dienes T, Fergenson D P, Prather K A, 1997. Real-time analysis of individual atmospheric aerosol particles: Design and performance of a portable ATOFMS. *Analytical Chemistry*, 69(20): 4083–4091.

Guenther A, Hewitt C N, Erickson D, Fall R, 1995. A global model of natural volatile organic compound emissions. *Journal of Geophysical Research*, 100(D5): 8873–8892.

Hao L Q, Wang Z Y, Huang M Q, Pei S X, Yang Y, Zhang W J, 2005. The size distribution of the secondary organic aerosol particles from the photooxidation of toluene. *Journal of Environmental Sciences*, 17(6): 912–916.

Jang M, Czoschke N M, Lee S, Kamens R M, 2002. Heterogeneous atmospheric aerosol production by acid-catalyzed particle-phase reaction. *Science*, 298(5594): 814–817.

Kroll J H, Ng N L, Murphy S M, Flagan R C, Seinfeld J H, 2006. Secondary organic aerosol formation from isoprene photooxidation. *Environmental Science and Technology*, 40(6): 1869–1877.

Kwok E S, Atkinson R, Arey J, 1995. Observation of hydroxycarbonyls from the OH radical-initiated reaction of isoprene. *Environmental Science and Technology*, 29(9): 2467–2469.

Miyoshi A, Hatakeyama S, Washida N, 1994. OH radical-initiated photooxidation of isoprene: An estimate of global CO production. *Journal of Geophysical Research*, 99(D9): 18779–18787.

Noble C A, Prather K A, 1996. Real-time measurement of correlated size and composition profiles of individual atmospheric aerosol particles. *Environmental Science and*

Technology, 30(9): 2667–2680.

Odum J R, Jungkamp T P W, Griffin R J, Flagan R C, Seinfeld J H, 1997. The atmospheric aerosol-forming potential of whole gasoline vapor. *Science*, 276(5309): 96–99.

Paulson S E, Flagan R C, Seinfeld J H, 1992. Atmospheric photooxidation of isoprene Part I: The hydroxyl radical and ground state atomic oxygen reactions. *International Journal of Chemical Kinetics*, 24(11): 79–101.

Pilinis C, Pandis S N, Seinfeld J H, 1995. Sensitivity of direct climate forcing by atmospheric aerosols to aerosol size and composition. *Journal of Geophysical Research*, 100(D9): 18739–18754.

Ruppert L, Becker K H, 2000. A product study of the OH radical-initiated oxidation of isoprene: formation of C_5-unsaturated diols. *Atmospheric Environment*, 34(10): 1529–1542.

Sanadze G A, 2004. Biogenic isoprene: A review. *Russian Journal of Plant Physiology*, 51(6): 729–741.

Schwartz J, Dockery D W, Neas L M J, 1996. Is daily mortality associated specifically with fine particles? *Journal of the Air and Waste Management Association*, 46(10): 927–939.

Stevens P S, Seymour E, Li Z J, 2000. Theoretical and experimental studies of the reaction of OH with isoprene. *Journal of Physical Chemistry A*, 104(25): 5989–5997.

Surratt J D, Murphy S M, Kroll J H, Ng N L, Hildebrandt L, Sorooshian A *et al*., 2006. Chemical composition of secondary organic aerosol formed from the photooxidation of isoprene. *Journal of Physical Chemistry A*, 110(31): 9665–9690.

Szmigielski R, Surratt J D, Vermeylen R, Szmigielska K, Kroll J H, Ng N L *et al*., 2007. Characterization of 2-methylglyceric acid oligomers in secondary organic aerosol formed from the photooxidation of isoprene using gas chromatography/ion trap mass spectrometry. *Journal of Mass Spectrometry*, 42(1): 101–116.

Thomas D S, Amy E W, Autumn R D, 2008. Isoprene emission from plants: Why and how? *Annals of Botany*, 101(1): 5–18.

Tuazon E C, Atkinson R, 1990. A product study of the gas-phase reaction of isoprene with the OH radical in the presence of NO*x*. *International Journal of Chemical Kinetics*, 22(12): 1221–1236.

Xia Z H, Fang L, Zheng H Y, Hu R, Zhang Y Y, Kong X H *et al*., 2004a. Real-time measurement of the aerodynamic size of individual aerosol particles. *Acta Physica Sinica*, 53(1): 320–324.

Xia Z H, Fang L, Zheng H Y, Kong X H, Zhou L Z, Gu X J *et al*., 2004b. Real-time measurement of chemical compositions of individual aerosol particles. *Chinese Journal of Analytical Chemistry*, 32(7): 973–976.

Yu J, Jeffries H E, Lacheur R M L, 1995. Identifying airborne carbonyl compounds in isoprene atmospheric photooxidation products by their PFBHA oximes using gas chromatography/ion trap mass spectrometry. *Environmental Science and Technology*, 29(8): 1923–1932.